

QUADRUPOLE SCAN EMITTANCE MEASUREMENTS FOR THE ELI-NP COMPTON GAMMA SOURCE

A. R. Rossi*, A. Bacci, I. Drebot, L. Serafini, INFN-MI, Milano

A. Mostacci, A. Giribono, Università di Roma “La Sapienza”, Roma

E. Chiadroni, C. Vaccarezza, A. Variola, INFN-LNF, Frascati (Roma)

V. Petrillo, M. Rossetti Conti, C. Curatolo, Università degli Studi di Milano & INFN, Milano

A. Cianchi, Università di Roma “Tor Vergata”, Roma

Abstract

The high brightness electron LINAC of the Compton Gamma Source at the ELI Nuclear Physics facility in Romania is accelerating a train of 32 bunches with a nominal total charge of 250 pC and nominal spacing of 16 ns. To achieve the design gamma flux, all the bunches along the train must have the designed Twiss parameters. Beam sizes are measured with optical transition radiation monitors, allowing a quadrupole scan for Twiss parameters measurements. Since focusing the whole bunch train on the screen may lead to permanent screen damage, we investigate non-conventional scans such as scans around a maximum of the beam size or scans with a controlled minimum spot size. This paper discusses the implementation issues of such a technique in the actual machine layout.

INTRODUCTION

The Gamma Beam Source (GBS) is an advanced source of up to 19.5 MeV Gamma Rays based on Compton back-scattering, i.e. collision of an intense high power laser beam and a high brightness electron beam with maximum kinetic energy of about 740 MeV [1]. The Linac will provide trains of bunches in each RF pulse, spaced by the same time interval needed to recirculate the laser pulse in a properly conceived and designed laser recirculator, in such a way that the same laser pulse will collide with all the electron bunches in the RF pulse, before being dumped. The final optimization foresees trains of 32 electron bunches separated by 16 ns, distributed along a 0.5 μ s RF pulse, with a repetition rate of 100 Hz.

Electron beam spot size is measured with optical transition radiation profile monitors. In order to measure the beam properties along the train, the screens must sustain the thermal stress due to the energy deposited by the bunches. Preliminary studies have shown that conventional Optical Transition Radiation (OTR) screens of Al-Si (e.g. SPARC [2]) will not sustain the smaller spot size foreseen for the nominal GBS beam. Reference [3] deals with the analytical studies as well as numerical simulations to investigate the thermal behavior of the screens impinged by the nominal bunch.

The critical point for thermal stress issues is when the beam is tightly focused as it happens in a quadrupole scan to measure Twiss parameters. Anyway such measurement (as well as the full 6D characterization of the beam [4, 5]) is

of utmost importance in a high brightness linac where the figure of merit is the ratio between the bunch charge and its squared normalized emittance [6].

This paper investigates the possibilities of non conventional quadrupole scans to avoid extreme focusing conditions and compare such scans to the standard approach.

EMITTANCE MEASUREMENT BY QUADRUPOLE SCAN

The quadrupole scan technique requires to collect a set Σ of transverse size measurements on a target, with different machine settings m , in order to retrieve the unknown beam Twiss parameters upstream the quads [7], allowing to calculate its emittance. Σ can be graphically represented as a plot of σ values as a function of m . For example, using the thin lens approximation and varying only one quad, $\sigma^2(m)$ is a parabola whose minimum is a direct measurement of the beam beta function.

The number of parameters involved in the practical implementation of the method is rather large and, to our knowledge, no systematic studies exist trying to assess the impact of all such details on the final emittance measurement results. Among those parameters we can mention:

- dimension and exact details of Σ ; for forming an overdetermined system the number of σ values must be greater than 3 but an optimal value of this parameter is not known. The same is true for the parameters realizing each machine setting m . In [7] it is found that the scan fails whenever Σ does not contain a minimum *and* some amount of measurement errors is included;
- for inverting the overdetermined system, a statistical approach must be employed. So far, the only approach used is fitting $\sigma(m)$ with a weighted least square method. However, least squares is known to be sensitive to outliers, i.e. it is not robust against errors, so a different, more sophisticated method could perform better;
- the weight assigned to each σ value in the fitting process, is typically proportional to the inverse of the variance associated to each spot measurement. Since such measurements, for practical reasons, are based on a rather small number of observations, both accuracy and precision may be poor. It is then unknown if, and to what extent, a better determination of the σ values

* andrea.rossi@mi.infn.it

and, hence, the associated variance could improve the result of emittance measurement.

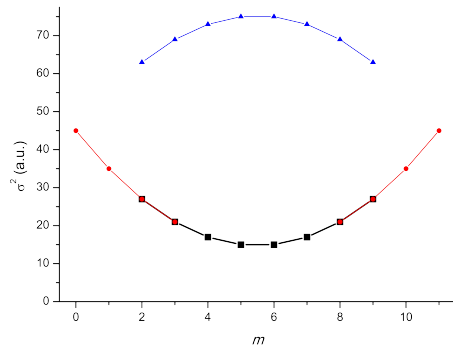


Figure 1: Pictorial result of quad scans settings: (a) scan with minimum (black squares), (b) scan with missing minimum (red circles) and (c) scan on a maximum (blue triangles).

EMITTANCE MEASUREMENT SIMULATIONS

In this section, we will analyze different settings for emittance measurement, Fig. 1, with different error levels; in particular, we focus on (a) the usual scan with minimum, (b) a scan where the minimum is missing and (c) a scan on a maximum.

In the following, σ_m will denote the exact theoretical value of the beam spot size on the screen, i.e. $\sigma_m^2 = [\mathbf{M}(m) \cdot \mathbf{v}]_{1,1}$, where $\mathbf{M}(m)$ is the transport matrix for machine setting m and $\mathbf{v} = (\alpha_T, \beta_T, \gamma_T) = (-2.36, 79.52, 0.12)$ the initial (unknown) beam Twiss parameters vector. The spot size value including experimental errors will be denoted by σ_i and is defined as $\sigma_i = \sigma_m (1 + \eta)$, where η is a normally distributed random variable with zero average and a standard deviation σ_η which is varied so that $\Lambda = \log_{10}(\sigma_e/\sigma_m) = -1, \dots, -6$ in steps of -1. The value employed for retrieving emittance is formed by calculating the average of $n_d = 10$ observations of σ_i and will be called $\langle \sigma \rangle_m$. Finally, the number of points employed in a scan, i.e. the dimension of Σ , will be denoted n_m . Each scan is then employed to retrieve an emittance values by a least square fitting process.

We performed a number $n = 10000$ scans for each setting and each error level. For settings (a) and (c) we set $n_m = 7$, while for setting (b) we set $n_m = 14$; notice, however, that for all settings, this parameter did not impact significantly on the retrieved emittance values provided that $n_m \geq 5$ and, for setting (b), that sigma data were evenly distributed around the missing minimum. For both settings (b) and (c), we set up the spot size measurements so that they returned a value larger than an arbitrary threshold of $100 \mu\text{m}$ while, for setting (c), the maximum turned out to be around $600 \mu\text{m}$; reducing the threshold value for setting (b) may result in a substantial performances improvement (depending on the amount of reduction), as setting (b) tents to setting (a), while reducing the maximum value for setting (c) only gives a

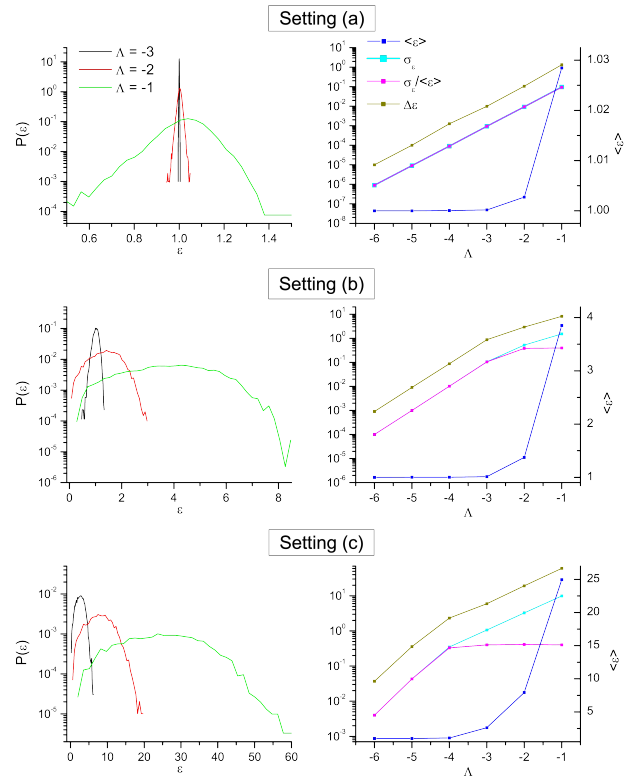


Figure 2: Probability density distribution functions (left column), distributions momenta (right column, right axis) and emittance results full spans (right column, right axis) for the three quad scan settings considered: (a) top row, (b) mid row and (c) bottom row

marginal performances enhancement. All retrieved emittance values have been normalized to the initial value of $\epsilon = 1.761 \mu\text{m}$; we then counted the number of occurrence for each value, $N(\epsilon)$, with an appropriate binning in ϵ . In order to better compare results, we calculated the probability distribution density $P(\epsilon)$ by normalizing $N(\epsilon)$ to the number of scans and the total span of emittance values $\Delta\epsilon$, i.e. $P(\epsilon) = N(\epsilon)/(n\Delta\epsilon)$. Results are reported in Fig. 2, left column, for all settings and error levels corresponding to $\Lambda = -3, -2, -1$. On the right column, for each setting, we plot the values of resulting distribution average $\langle \epsilon \rangle$ value, standard deviation σ_ϵ , relative width $\sigma_\epsilon/\langle \epsilon \rangle$ and retrieved emittance values full span $\Delta\epsilon$.

We start noticing that setting (a), on average, remains accurate and precise for all error levels, although a slight drift, around 3%, of the distribution maximum toward higher emittance values is present (Fig. 2, top line). The distribution itself retains a Gaussian shape up to 1% error level (left plot, black and red lines) and starts to be a bit asymmetric for higher errors (green line). In this last situation, the worst results may be off by as much as 40%, although their probability is extremely low. Moreover, distribution moments and full span of results turn out to be roughly a linearly increasing function of error level (right plot). Finally, when $\Lambda = -1$, we had two out of 10000 inconsistent retrieved emittance

values (i.e. $\epsilon^2 < 0$), coming from particularly overall inaccurate scans (see Table 1). Those values were rejected and not included in the subsequent analysis. We conclude confirming that setting (a) is robust against stochastic errors even of relevant relative magnitude.

Table 1: Number of Inconsistent (Failed) Measurements for each Setting and Error Level

Setting	-6	-5	-4	Λ	-2	-1
a	0	0	0	0	0	2
b	0	0	0	0	3132	4840
c	0	0	1199	4539	4856	4973

On contrary, setting (c) displays a high sensitivity to errors even when they are as small as few per mil and less, Fig. 2, bottom line. The emittance values distributions are non-Gaussian starting from $\Lambda = -3$ and a considerable drift of all distributions moments toward higher than reliable values occurs as soon as the percent error level exceeds 0.01% (left plot). Above that threshold, moments are non longer linear functions of errors, while the relative distribution width approaches a limiting value close to 0.4 (right plot). This means that σ_ϵ scales like $\langle \epsilon \rangle$ as occurs, for example, in a Gamma distribution. The motivation of this behavior is not clear and could be possibly a consequence of the high number of inconsistent outcomes that roughly approaches 50% of the total measurements starting from the threshold, see table 1.

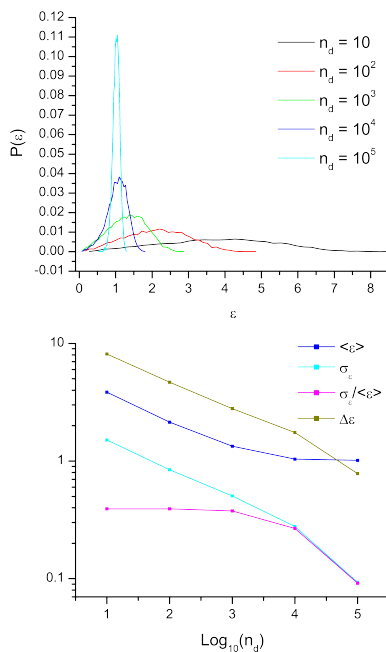


Figure 3: Probability density distributions for an increasing number of σ observations n_d (top) and scaling of the distributions momenta and full emittance results span (bottom).

Finally, setting (b), Fig. 2 mid column, has performances laying in between the other two settings and the threshold for reliable emittance measurements is set at $\Lambda = -3$, meaning a .1% error level. This precision may be reached with an extremely stable machine but constitute, in general, a challenge.

In order to improve results reliability, we tried to implement robust methods in determining both the values of $\langle \sigma \rangle_m$, by calculating the median of σ_i instead of the average, and in the fitting process, making use of M-estimators (see, for example, [8]). The results (not reported) show that we can get an improvement of a variable factor between 1 and 3, in terms of distribution moments, for settings (b) and (c); although this may be relevant in some specific situations, it is not enough in general.

In our simulations, we set the number of observations for determining $\langle \sigma \rangle_m$ equal to 10. This is because, in a 10 Hz repetition rate linac, that value allows to perform an emittance measurement in few minutes. However, the ELI-NP Compton sources operates at 100 Hz, so that a more accurate measurement of $\langle \sigma \rangle_m$ is feasible employing a larger value of n_d . In order to check if this solution can effectively improve emittance measurements, we repeated the simulations for setting (b) with $\Lambda = -1$ and an increasing number of observations for determining $\langle \sigma \rangle_m$. The results are shown in Fig. 3. The top plot shows how the probability density distribution is modified by n_d ; we notice how both accuracy and precision can be significantly improved by increasing n_d . The bottom plot displays the distributions momenta and emittances full span, showing that the threshold for reliable emittance measurements depends on the accuracy in the measurement of $\langle \sigma \rangle_m$ and how, for $\Lambda = -1$, it moves somewhere between $n_d = 10^3$ and $n_d = 10^4$. As a further confirmation of that, the number of inconsistent results, which is around 50% with $n_d = 10, 10^2$, drops to less than 5% for $n_d = 10^4$ and is zero for $n_d = 10^5$. Although this last value is not feasible with a 100 Hz repetition rate, a full scan with $n_d = 10^4$ would require ten to fifteen minutes to perform, provided the acquired data are managed with adequate speed.

CONCLUSIONS

In this paper we performed a systematic study of emittance measurements by quadrupole scans in different settings, some of them aimed at preventing permanent damages to OTR screens when high power electron beams are involved. We proposed quadrupole scans not including the heavily focused beam as well as scans including a maximum of the beam spot size. We investigated how stochastic errors affecting the measurements of beam spot affect the evaluation of emittance and found that a setting dependent threshold do exist for reliable measurements. We also demonstrated that, within one setting and a given error level, the threshold depends on the accuracy with which the spot is measured and a high accuracy allows to get reliable emittance results also with non standard scan settings.

REFERENCES

- [1] A. Bacci *et al.*, “Electron Linac design to drive bright Compton back-scattering gamma-ray sources”, *J. App. Phys.* **113**, 194508 (2013).
- [2] A. Bacci *et al.*, “Status of Thomson source at SPARC/PLASMONX”, *Nuc. Inst. Meth. Phys. Res. A* **608**, S90 (2009).
- [3] M. Marongiu *et al.*, “Design Issues for the Optical Transition Radiation Screens for the ELI-NP Compton Gamma Source”, presented at IPAC’16, Busan, Korea, May 2016, paper MOPMB017.
- [4] A. Cianchi *et al.*, “Six-dimensional measurements of trains of high brightness electron bunches”, *Phys. Rev. STAB* **18**, 082804 (2015).
- [5] D. Filippetto *et al.*, “Phase space analysis of velocity bunched beams”, *Phys. Rev. STAB* **14**, 092804 (2011).
- [6] C. Vaccarezza *et al.*, “Optimization Studies for the Beam Dynamic in the RF Linac of the ELI-NP Gamma Beam System”, presented at IPAC’16, Busan, Korea, May 2016, paper TUPOW041.
- [7] A. Mostacci *et al.*, “Chromatic effects in quadrupole scan emittance measurements”, *Phys. Rev. STAB* **15**, 082802 (2012).
- [8] P.J. Huber, *Robust Statistics*, 2nd edition, Hoboken, NJ: John Wiley & Sons Inc. ISBN 978-0-470-12990-6.